Mechanical energy harvesting, storage and utilization methods and devices are a little explored area with a potential to replace electrical energy in machines operated with electricity and which is environmentally friendly. Energy harvesting from human actions is an optimistic solution to provide energy supply. There are various methods and techniques that discuss energy harvesting from human actions. The problem is that most of these methods deal with tiny energy output. The object of this study is to design and characterize a flat spiral spring based method to harvest enough mechanical energy, to store and to drive a ride as in an amusement park instead of electricity. A flat spiral spring is specifically designed and fabricated for this purpose. To begin with, a life-size prototype of the kids' ride using the flat spiral spring is modeled, analyzed, fabricated and implemented on the kids' ride prototype. The stability of the ride is analyzed by modeling the impact of the collision between two kids' rides. Energy is harvested by winding the spring by hands using a handle or by pulling back the kids' ride and is stored in the spring. Experimental results show that the proposed method of harvesting, storing and utilization of mechanical energy can be an alternative to electrical energy in operating high-power machines like kids' rides. An optimum width of 30 mm and a thickness of 1.4 mm for the flat spiral spring are found to help in ease of manufacturability, ease of rotation by human and compactness. The average force required to wind the spring is calculated to be 16.06 N, which is approximately 33 % of the force that can be exerted by a human hand. The stability of the proposed system in case of collision is verified by calculating the roll angle, which is less than 3.83 degrees, which is well below the recommended roll angle limit in case of collision

Keywords: mechanical energy harvesting, alternative to electricity, energy conversion, flat spiral spring, kids' ride

UDC 265224
DOI: 10.15587/1729-4061.2022.265224

DEVELOPMENT OF A METHOD TO HARVEST MECHANICAL ENERGY TO USE AS AN ALTERNATIVE TO ELECTRICAL ENERGY IN ELECTRIC POWERED RIDES

Rajesh Kannan Megalingam
Corresponding author
Doctor of Philosophy (ECE), Director, Associate Professor*
Humanitarian Technology (HuT) Labs**
E-mail: rajeshm@am.amrita.edu
Bharath Sasikumar
Bachelor of Technology in Mechanical Engineering,
Research Assistant*
Dhananjay Raghavan
Master of Science in Aerospace Engineering,
Associate Senior Research*
Shree Rajesh Raagul Vadivel
Master of Technology in Digital Manufacturing, Robotics Engineer*
Sreekanth Makkal Mohandas
Master of Technology in VLSI Design,
Research Associate*
Sakthiprasad Kuttankulangara Manoharan
Doctor of Philosophy Scholar*
Humanitarian Technology(HuT) Labs**
*Department of Electronics and Communication Engineering**
**Amrita Vishwa Vidyapeetham
Engineering College Road, Kollam, India, 690525

Received date 06.09.2022
Accepted date 18.11.2022
Published date 30.12.2022
How to Cite: *Megalingam, R. K., Sasikumar, B., Raghavan, D., Raagul Vadivel, S. R., Makkal Mohandas, S., Kuttankulangara Manoharan, S. (2022). Development of a method to harvest mechanical energy to use as an alternative to electrical energy in electric powered rides. Eastern-European Journal of Enterprise Technologies, 6 (7 (120)), 54–62. doi: https://doi.org/10.15587/1729-4061.2022.265224*

1. Introduction

The amusement parks industry is one of the world's fastest-growing industries in terms of revenue collected and attendance per year. In India, the size of the amusement parks business is estimated to be about 534 million USD and is expected to grow by an additional 10 percent in the coming years [1]. In other developing countries, amusement parks and entertainment centers are major assets of the tourism industry. Although the financial benefits and GDP contribution of the tourism industry are high, the environmental impact of these industries has gained widespread attention, especially in countries with limited natural resources [2]. Though initially introduced for kids, modern-day amusement parks consist of high-speed, high-altitude rides meant for adults as well. For ease of understanding, parks have been classified into three categories based on the number of rides in each. Category I rides (high-power) include roller coaster, circular rides and thrill rides with annual electricity consumption of 175 MWh, 233 MWh and 131 MWh, respectively. Ferris wheels, swing, carousels, water rides, and kids swing are part of Category II rides (medium-power) with annual electricity consumption of 58 MWh, 43 MWh, 40 MWh, 35 MWh and 29 MWh, respectively. Category III rides (low-power) include transportation rides, kids track rid, virtual reality games, bumper cars, kiddie rides with annual electricity consumption of 11 MWh, 1.4 MWh, 876 KWh, 759 KWh and 175 KWh, respectively. 500 MWh of power is consumed by high-power rides annually on average. Circular rides among high-power rides consume about 233 MWh power annually. The combined power con-

sumption of category I rides is more than two times that of category II rides, which are medium-power rides and 166 times that of category III rides. Kids' rides are categorized as low-power rides, which consume 3 MWh of power per year. Even though low-power rides consume much less power compared to the other two categories, still it becomes a significant amount of power when thousands of amusement parks across the world are taken into account. Even though we couldn't compile data of all the amusement parks in the world, the compiled list of eight amusement parks gives a glimpse of the dire power requirements of kids' rides among all other rides.

Hence there is a need for developing alternative sources of energy instead of electricity. While there are alternative sources of energy like solar, wind, etc., converting mechanical energy created by human actions into electrical energy is the easiest. Mechanical energy is distributed and present almost everywhere in our surrounding environment [3, 4]. It can be generated from human motion [5], automotive [6], airflow [7], waterway [8], and mechanical equipment [9]. Therefore, studies on using electric energy as a source of power in which energy generation is mostly thermal or nuclear, which leaves irreparable damage to the environment, are of scientific relevance.

2. Literature review and problem statement

The paper [10] presents the results of research on harvesting the waste energy of vehicles using a mechanical system built in the decelerating downhill roadways. Though energy harvesting efficiency is only 40 %, vehicles don't always decelerate downhill. In addition, the mechanism built for harvesting energy is complex and costly. The paper [11] proposed the results of a novel polydimethylsiloxane (PDMS) based triboelectric generator (TEG) to convert wasted mechanical energy into electrical energy, which can be used only for low-power electronic applications. Hence this method is not suitable for high-power applications. The paper [12] presents the results of research to improve power absorption in ocean wave energy converters. Though the proposed method improves efficiency as claimed by the authors, the method and implementation are very complex. The paper [13] presents the results of research on harvesting energy from the human wrist motion while walking, running and jogging using a sprung eccentric rotor. But the generated energy is very tiny, in the range of a few microwatts, which is not suitable for even low-power electronic applications.

A piezoelectric based energy harvester is demonstrated in [14], which can generate a few hundred of microwatts power. Though the proposed research work yields better results compared to [13], it is still not enough for high-power machines like electric rides. The paper [15] presents the results of research on generating power from human walking. Though the method could generate power in the range of a few milliwatts, harvesting energy from human walking to power electric rides is an exhaustive and impractical method. The research work proposed in [16] presents a vibration energy harvester from human walking yielding better energy harvesting in the range of hundreds of milliwatts of power compared to [15]. The power generated can be only used for low-power applications. The paper [17] presents the results of research on harvesting energy from human motion via nanogenerators to be used in wearable devices only. The method proposed in this research work is not suitable for electric rides, which consume a lot of power.

The results presented in the research work [18] indicate a huge loss of power when mechanical energy is converted into electrical energy, which is as much as 70 % and the power output is also very small in the range of a few tens of microwatts. Our earlier work on energy focused on converting pedal power into electrical energy for lighting rooms [19]. But this method cannot be used for electric rides as a person constantly needs to ride. In another work [20], we proposed a solar-powered water pumping system for eco-friendly irrigation, which uses electricity from solar energy to power the pump. Due to energy conversion, there is a loss of energy in this method. Moreover, the efficiency of solar panels is less than 40 % and the implementation is associated with high costs. The results discussed in the research work [21, 22] are similar to [19], and hence impose the same limitations as that of [19]. The wind energy conversion method presented in [22] is very complex and difficult to implement.

All the proposed methods of harvesting mechanical energy focuse on low-power applications in which mechanical energy is converted into electrical energy, which is used to operate electronic devices. Moreover, they are not scalable, and the design complexity makes them much harder to be used for high-power applications. In addition, as electrical energy is used as primary energy to operate these devices, there is going to be a considerable amount of greenhouse gases generated while operating these devices. This suggests that there is a strong need to conduct research focusing on harvesting energy, which can be used for high-power machines like electric rides, which is clean and doesn't generate greenhouse gasses. The method thus developed should be stable and safe to use. It should be able to generate energy with simple human actions. The developed technology should adhere to ease of manufacturability and ease of handling by humans.

3. The aim and objectives of the study

The aim of the study is to develop a method to generate mechanical energy, which when used to drive high-power devices doesn't generate greenhouse gases and is safe for the environment.

To achieve this aim, the following objectives are accomplished:

– modeling, analyzing, and fabricating a kids' ride called Turtle Bot Ride (TBR), which uses a flat spiral spring and a gear system to drive the ride along with a mechanism to input energy from human actions;

– analyzing the impact of the collision between two kids' rides;

– calculation of the optimum width and thickness of the flat spiral spring for identifying the ease of manufacturability, ease of rotation by human and compactness and validation of the spring specifications using simulations and real-time testing with TBR;

– calculation of the amount of force a person has to exert in order to wind the spring to the maximum count to determine if TBR can be easily operated by humans.

4. Material and methods

The TBR design consists of five major elements integrated into the turtle bot body. These include a flat spiral spring that forms the core element of the design, a gear set, as well as a chain

and sprocket that helps in power transmission and the crank and slot mechanism for the yaw motion in the head and tail.

Fig. 1 shows the exploded view of the assembly of the mechanism responsible for the motion of the turtle bot kids' ride. At the right top corner of Fig. 1, there is the complete assemble turtle bot view. The entire mechanism sits inside a turtle-shaped chassis (13) with a head (10) and a tail (11). In the design, the spiral spring (1) is the main energy storage element. The spring arbor shaft (2) extends out of the gear-box chassis (14). The end of the shaft has a rectangular cross section that meshes with a rectangular slot on the handle (4). The other end of the handle has a rotatable grip (5) mounted on a deep groove ball bearing (6). The other end of the spring arbor shaft extends towards the other side to mount the main large gear (7). The main transmission system consists of two other gears and a chain and sprocket system (9) for further torque reduction. The smallest gear transmits the drive torque to the front wheels (8) while the medium gear connects to a crank slot (12) mechanism that causes the head (10) and tail (11) to yaw like in an amusement park kids' ride. The calculations and parameters for choosing the components have been discussed later in the paper.

An off-the-shelf sprocket and chain system transfers the energy from the gear to the wheels. The flat spiral spring unwinds quickly transferring power to the wheels causing them to accelerate. Once the spring unwinds fully, the gears would stop rotating and the wheels would lock up instantly. Including the chain and sprocket in the design ensures that the wheels will keep rotating freely thereby increasing the distance covered. As the model is intended to be a kids' ride, a simple head and tail yaw motion via a crank slot mechanism is included for fun. The crank is mounted on the same shaft as the medium gear. In addition, the slot is on a mild steel strip connected to the pivot axis of the head and tail and a lighter stainless steel (SS) pipe connected to the crank (by a horizontal rod) runs through the slot. When the crank rotates, the SS pipe moves up and down through the slot pivoting the head and tail about their respective axes.

To calculate the net energy conversion and consumption, we find out the equations of motion and prepare the mathematical model of the system using the constrained Euler-Lagrange method. Fig. 2 shows the free body diagram of the turtle robot.

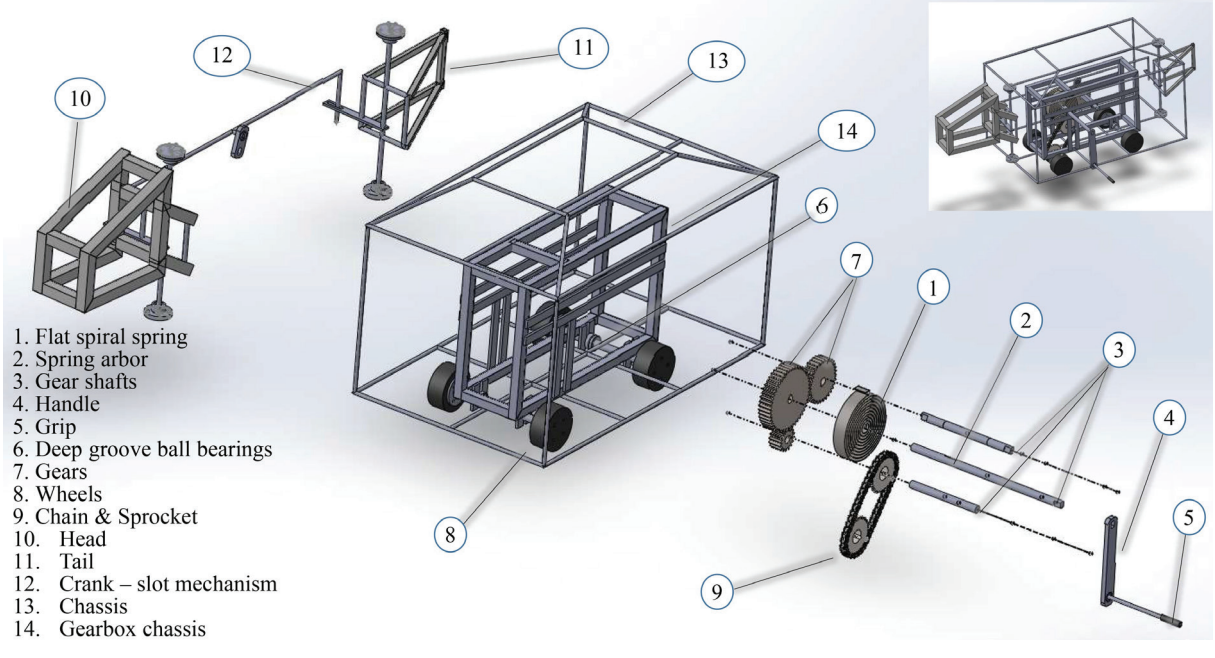

Fig. 1. Design principle of the mechanical energy harvesting and utilization mechanism using a flat spiral spring — exploded view

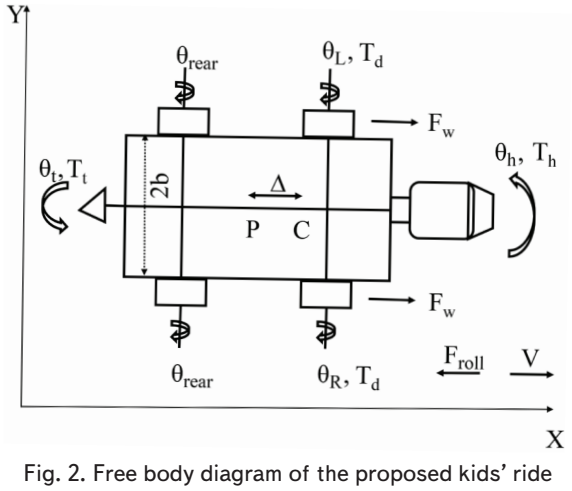

Fig. 2. Free body diagram of the proposed kids' ride

We assume that the various losses such as transmission losses, frictional losses, etc. are minimized and the total potential energy is converted to the kinetic energy of the system. Since the energy storage element in the system is the flat spiral spring, the potential energy of the system would be the elastic potential energy or the strain energy of the metal strip. Even though the equation for constructing the flat spiral spring is readily available, we aim to develop the mathematical modeling of a system powered by such a spring.

5. Results of research on harvesting mechanical energy to use as an alternative to electrical energy

5. 1. TBR Modelling

All the forces and motions of the body are marked in the free body diagram. The purpose of our mathematical modeling is to find out the equations that govern the motion of a four-wheeled vehicle with a two-wheel drive and head and tail components in oscillation. Table 1 shows the definition of symbols used in this section.

The system has a mass m_p, width $2b$, and center of gravity at x_c. The head and tail components rotate with angles θ_h and θ_t, respectively. The body of the system (excluding the head and tail) has a center of gravity at x_p and velocity of the center of gravity of $\dot{X}_p$:

$$L=\frac{1}{2}m_pX_P^2+\frac{1}{2}I_w\dot{\theta}_R^2+\frac{1}{2}I_w\dot{\theta}_L^2+\frac{1}{2}I_T\dot{\theta}_T^2+\frac{1}{2}I_H\dot{\theta}_H^2. \quad (1)$$

Since the spring and gears are connected to the front wheel shaft, the dynamics of the turtle bot is related to the dynamics of the front wheel drive vehicle. Hence, it is similar to a front wheel vehicle. The rear wheel angle θ_{rear} equals to zero since it is not powered and is omitted. Once we have a proper free body diagram, we note down all the rotations and translations and form the Lagrangian L. The use of energies and generalized coordinates in the Lagrangian model is more favorable for us in this case rather than the forces and constraints in the Newtonian model. Since,

$$X_c=X_p+\Delta,\ \dot{X}_P=\dot{X}_C. \quad (2)$$

Here, we assume that the turtle bot has two pairs of wheels facing straight and can move in a straight line on being powered. The spring and the transmission deliver power linearly to the front wheel shaft connecting the two wheels. Hence, the rotation of the two front wheels is equal. On differentiating the Lagrangian L with the four coordinates x_c, θ, θ_H and θ_T, we get the equations,

$$\dot{m}_p\ddot{X}_c=2F_w-F_{roll}, \quad (3)$$

$$I_w\ddot{\theta}_L=I_w\ddot{\theta}_R=T-rF_w. \quad (4)$$

The driving torque in the system would be the torque T_d supplied by the flat spiral spring when it is wound to θ_S radians. The equation for the torque is readily available and has been used to obtain numerical values. The frictional force F_w on the front wheels provides the traction required for the motion. Since the right and left wheels rotate with the same angular acceleration, we assume the term $\theta=\theta_R=\theta_L$. Hence,

$$I_w\ddot{\theta}=T_d-rF_w, \quad (5)$$

Now, $F_w=\frac{m_p\ddot{X}_c}{2}$, and since, $\dot{X}_c=r\dot{\theta}$, $\ddot{X}_c=r\ddot{\theta}$.

Table 1

Symbols Table

Symbols	Definition
θ_R	Right wheel rotation angle, radians
θ_L	Left wheel rotation angle, radians
T_d	Driving torque, Nm
θ_h	Angle of deflection of head, radians
T_h	Torque for head yaw, Nm
l	Length of spring metal strip, m
t	Thickness of strip, m
θ_{rear}	Angle of deflection of rear wheels, radians
θ_S	Spring winding angle, radians
V	Forward velocity of system, m/s
C	Center of gravity of entire system
x_c	Position of center of gravity of entire system
$\dot{X}_c$	Velocity of center of gravity of entire system
$\ddot{X}_c$	Acceleration of center of gravity of entire system
P	Point of collision
h	Height of P from ground
C	Center of mass of vehicle
a	Height of C from ground
M_t	Toppling moment
M_s	Stabilizing moment
F_W	Frictional force on front wheels, N
F_{roll}	Rolling resistance on rear wheel, N
T_t	Torque for tail yaw, Nm
θ_t	Angle of deflection of tail, radians
$2b$	Width of turtle bot body
T_s	Torque from spring, Nm
m_p	Mass of turtle bot body, kg
C_{rr}	Coefficient of rolling resistance
I	Moment of inertia, kg·m^2
P	Center of gravity of turtle bot body
Φ	Angle of inclination of R w.r.t ground
x_p	Position of center of gravity of turtle bot body
$\dot{X}_p$	Velocity of center of gravity of turtle bot body
r	Moment arm for stabilizing moment
m	Mass of vehicle
b	Half-track width of vehicle
φ	Roll angle
Δ	Distance between P and C
g	Acceleration due to gravity
R	Distance between CG and pivot point

As the turtle bot moves on a surface, the wheels rolling over it will experience a drag or a rolling resistance. This rolling resistance is caused by inelastic forces and is a function of the mass of the body. The coefficient of rolling resistance is based on the standard friction equation and often depends on the type of wheel and the surface on which it moves. Rolling resistance $F_{roll}=m_p*g*C_{rr}$. Substituting and simplifying

$$I_\omega\frac{\ddot{X}_c}{r}=T_d-\frac{rm_p\ddot{X}_c}{2}-\frac{rF_{roll}}{2}, \quad (6)$$

$$\ddot{X}_c = \frac{T_d - \frac{rF_{roll}}{2}}{\frac{I_\omega}{r} + \frac{rm_p}{2}}. \quad (7)$$

(7) gives the acceleration of the center of gravity of the entire system. Thus, equations 2 to 7 in the proposed mathematical modeling govern the motion of a TBR four wheeled vehicle, with two-wheel drive and head and tail components in oscillation.

5. 2. Collision Analysis

The analysis of the impact of the collision between two kids' rides is very important to make sure that the proposed kids' ride is safe for kids. While riding the proposed turtle bot, there is a possibility that one kids' ride collides with another while the kids are seated. In such a scenario, impact due to the collision should not cause an accident and hurt the kids. We assume that there are two kids' rides; *A* and *B*. Ride *A* hits ride *B*. Fig. 3 shows the front view of ride *B* of mass '*m*' after it was hit in the side by ride *A*. Ride *A* is not shown in the figure. The point of impact is *P*, at a height of '*h*' from the ground and the CG (center of gravity) of vehicle *B* is assumed to be at point *C*, at a height of 'a' from the ground. Due to the collision, vehicle *B* tilts by an angle φ, and tends to roll over about the *Z*-axis at the CG due to the momentum transfer. Ride *A* collides with the side of ride *B* of the same size and mass (T-bone collision). The point of impact is *P*, at height '*h*' from the base of the ground. Vehicle *B* does not slip to the side, instead starts to roll over about its left wheel. Upon collision, ride *A* transfers a force equal to its rate of change of momentum to *B*. This applied force creates a toppling moment about the CG in *B*.

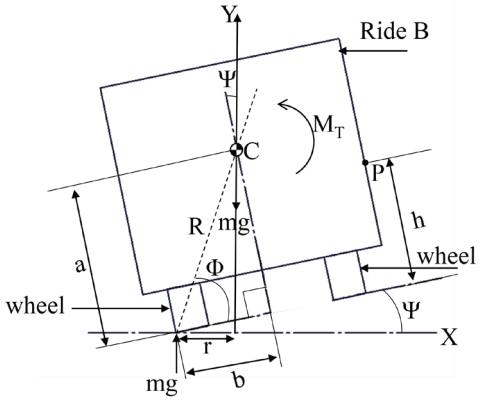

Fig. 3. Collision diagram of the proposed kids' ride when it is hit by another proposed kids' ride operating in the same arena

Toppling force $F_t = m\frac{dv}{dt}$.

Toppling moment $M_t = m\frac{dv}{dt}(h-a)$.

The weight of the body offers a stabilizing moment about the CG.

Stabilizing moment, $M_s = mg*r$.

Now, from the Fig. 3, $R = \sqrt{a^2+b^2}$.

$$\phi = \tan^{-1}\left(\frac{a}{b}\right).$$

Now, the horizontal moment arm for stabilizing moment,

$$r = R\cos(\Phi+\varphi) = \sqrt{a^2+b^2}\cos\left[\tan^{-1}\left(\frac{a}{b}\right)+\varphi\right].$$

For stability,

$$M_t < M_s,\ m\cdot\frac{dv}{dt}(h-a) < m.g.r.,$$

$$\frac{dv}{dt}\cdot\frac{(h-a)}{g\sqrt{a^2+b^2}} < \cos\left[\tan^{-1}\left(\frac{a}{b}\right)+\varphi\right], \quad (8)$$

$$\left[\tan^{-1}\left(\frac{a}{b}\right)+\varphi\right] < \cos^{-1}\left(\frac{dv}{dt}\cdot\frac{(h-a)}{g\sqrt{a^2+b^2}}\right), \quad (9)$$

$$\varphi < \cos^{-1}\left(\frac{dv}{dt}\cdot\frac{(h-a)}{g\sqrt{a^2+b^2}}\right) - \left[\tan^{-1}\left(\frac{a}{b}\right)\right]. \quad (10)$$

For the proposed turtle bot, a=255 mm, b=155 mm, h=300 mm. Assuming the 'g' force will be less than that of other amusement park rides like roller coaster, a value of 3g deceleration during collision is taken [23, 24].

$dv/dt = 30\ \text{m/s}^2$.

φ<3.83 degrees.

This is well below the recommended roll angle [22] limits for vehicles. Thus, the stability of the design in side impact collisions is verified.

5. 3. Calculation of the optimum width and thickness of the flat spiral spring

Since a comfortable acceleration for a seated adult is 0.2g [14], we assume a safety factor of 3 (for kids) and set a maximum acceleration limit of 0.65 m/s^2.

Assuming C_{rr}=0.025 (rubber on tarmac), F_{roll}=5 N. Substituting the values of $\ddot{X}_c = 0.65\ \text{m/s}^2$, r=0.05 m, m=25 kg, F_{roll}=5 N, I_ω=0.0002474 kg·m^2, Max T_d=2.88 Nm.

[8] equates the elastic potential energy of the spring to the strain energy of a bent metal strip and gives the relation,

$$\theta = \frac{12Tl}{Ebt^3}. \quad (11)$$

The research work [25] concludes that the flat spiral spring cannot remain stable after three full turns, the maximum angle of rotation is taken as 6π radians or 1080 degrees. The auxiliary head and tail yaw motion is only for entertaining kids and requires about one-fifth of the driving torque. The net torque to be produced by the spring adds up to about 3 Nm. The energy from the spring reaches the wheels through a transmission system having a gear drive so as to ensure that the spring unwinds in a controlled manner over a longer period of time. Further, a chain drive with freewheel is also incorporated into the design to ensure that the wheel keeps rolling freely due to momentum and does not lock up immediately after the spring unwinds fully.

Considering the application and availability, gears and chain drive of the following specifications are selected: the

designed gearbox comprises ~~of~~ three gears for two separate single stage reductions:

Spring to wheel: single stage reduction.
Gear 1: 60 teeth, module=2.
Gear 2: 20 teeth, module=2.
Spring to crankshaft: single stage reduction.
Gear 1: 60 teeth, module=2.
Gear 2: 40 teeth, module=2.
Transmission ratio of gear drive: 3:1.
Chain Specifications: standard BSA Hercules freewheel and chain are used.
Free wheel: 18 teeth.
12.7 mm pitch.
3.2 mm width.
Chain: 12.7 mm pitch.
3.3 mm width.
Transmission ratio of chain drive: 1.5.
Net transmission ratio=4.5.

Considering the transmission ratio, the net torque to be produced by the spring T_s=13.5 Nm. Substituting the values of E=209 GPa, T=13.5 Nm, θ=6π,

$$\frac{bt^3}{l} = 4.11\times10^{-11} \text{ m}. \quad (12)$$

From (9), we can observe that as the thickness of the spring (t) increases, the spring becomes stiffer and harder to manufacture and wind. Also, as the width (b) increases, the spring becomes less compact. Hence, choosing an optimum width and thickness becomes important. For the same, a table of possible widths, thicknesses and corresponding length values is prepared and shown in the supplementary file.

Considering availability and manufacturability, a spring of the following specifications is manufactured:

Flat spiral spring:
Material: EN 42 spring steel.
Width: 30 mm.
Thickness: 1.4 mm.
Length: 2 m.

5. 4. Validation of spring specifications via simulations and using TBR

MATLAB simulations are carried out for validating the spring specifications. Since the spring unloads rapidly, the torque from the spring is given as an impulse force acting for the first one second and zero for the rest of the simulation time. The displacement characteristics of the spring indicate that the displacement increases with time, which is as expected and reaches a peak value of 5.7 m when spring energy is exhausted, and the bot stops. In two seconds, the displacement is about 50 % percent of the 5.7 m peak value. This is due to changes in velocity caused by the spring. The velocity characteristics show that the peak velocity of 1.5 m/s is attained by the turtle bot in 1 second and the velocity is reduced to zero at the 7th second. The spring when released after winding to a maximum releases high energy in the beginning, which reaches a peak at 1 second and the energy keeps reducing from 1 second till 7 seconds when it becomes zero and the bot stops. Accordingly, the velocity increases and reaches a peak at 1 second and dies down at 7 seconds.

For the maximum number of turns of the flat spiral spring, the distance traveled by the turtle bot and the velocity are measured for four different load conditions:

a) no load;
b) 10 kg;
c) 20 kg; and
d 30 kg.

The load of 10–30 kg helps to find the behavior of the turtle bot when used by kids. Fig. 4 illustrates the distance traveled by the turtle bot for various load conditions. Fig. 5 illustrates the velocity profile for various load conditions. Each of the load characteristic curves is obtained by taking an average value of 10 iterations.

The simulation results match well with the performance test results indicating that the proposed design could work well with the load conditions for which it is designed. When the flat spiral spring is wound and released, the turtle bot started to move at a slow speed for around 1 m distance. Then it accelerates quickly and reaches maximum speed. For the distance characteristics shown in Fig. 4, as the load increases, the distance traveled by the turtle bot decreases. For no load and 10 kg load conditions, the bot could travel an average distance of 4.4 m, whereas for a 20 kg load, the bot could travel only up to 3.8 m. For a 30 kg load, the bot could travel a distance of 3.2 m only, on average.

In Fig. 5, for no load conditions, the velocity curve exhibits a linearity portion up to 0.9 s and the velocity reaches a maximum in 1.2 s at 2 m/s. The speed gradually reduces and reaches zero. Under various load conditions, the velocity curve exhibits a linearity portion up to 1.2 s for 10 kg and 20 kg loads, whereas the linearity portion extends up to 1.9 s for a 30 kg load. For a 10 kg load, velocity peaks at 1.7 m/s and for a 20 kg load, it peaks at 1.3 m/s, whereas for a 30 kg load, it is reduced to 1.1 m/s.

Table 2 shows the results of the experiment in which the torque required for winding the spring is measured. We want to find out how much force a person has to exert in order to wind the spring to the maximum count. In general, it is suggested that the adult human hand forces should not exceed 45 N when handling loads.

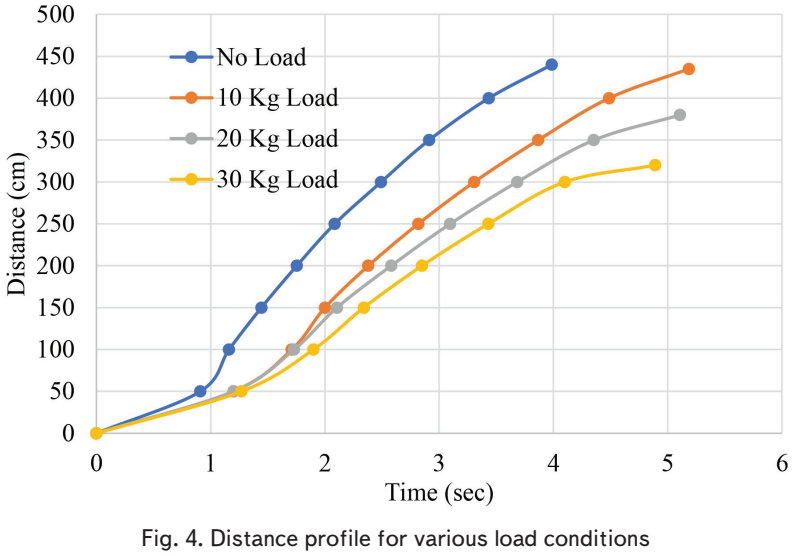

Fig. 4. Distance profile for various load conditions

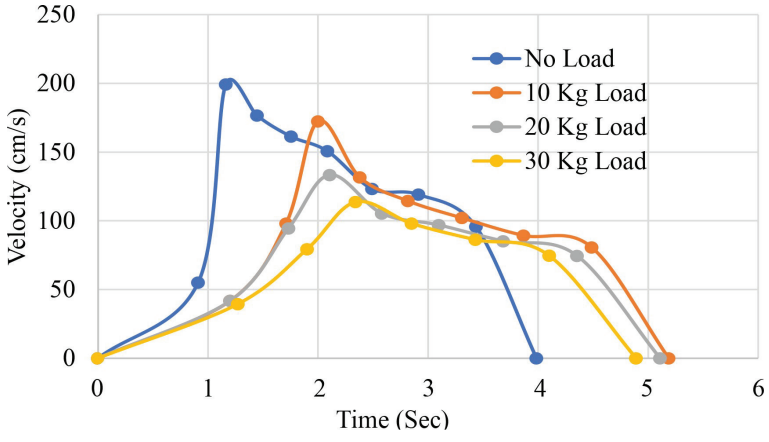

Fig. 5. Velocity profile for various load conditions. For similar conditions as in Fig. 4

Table 2

Observation Table – Angle Vs Loading Torque

Sl. No.	Angle of twist, Θ	Average Force, N	Torque, Nm
1	90	1.96	0.343
2	180	2.48	0.434
3	270	4.32	0.756
4	360	5.12	0.896
5	450	6.08	1.064
6	540	8.32	1.456
7	630	9.48	1.659
8	720	10.76	1.883
9	810	12.56	2.198
10	900	13.42	2.345
11	990	15.18	2.656
12	1,080	16.06	2.815

Initially, the person has to wind up the spring by using the handle as shown in Fig. 1, and then release in order to drive the TBR. In order to carry out this experiment, the outer end of the handle is connected to a weighing scale and the handle is rotated in a step of 90 degrees till it is rotated to a maximum of 3 rotations. Each 90-degree step rotation is repeated five times and the average force is listed in Table 2. The length of the handle is 17.5 cm. It is observed in Table 2 that for a maximum of 3 rotations of the handle, the average force required is 16.06 N, which is approximately 33 % of the force that can be exerted by a human hand. This proves that the TBR is easy to be driven by an adult.

6. Discussion of the results of the design, development, and implementation of TBR to harvest mechanical energy and operate high-powered machines

The focus of this study is to design, develop, and analyze a method to harvest mechanical energy to use as an alternative to electrical energy in electric-powered rides. The uniqueness of the proposed method is that it doesn't convert mechanical energy into electrical energy to operate electric rides thereby avoiding any loss in energy during conversion. Only clean mechanical energy is used to drive the rides. There is zero emission of greenhouse gases and zero damage to the environment.

The proposed method harvests energy from human action, which can power kids' rides used in theme parks. The flat spiral spring used for storing the mechanical energy from human action is analyzed and validated to be used in kids' rides. The analysis in subsection 5.3 shows that the spring width should be 30 mm and thickness 1.4 mm to avoid spring stiffness and make winding easier. The displacement characteristics of the TBR simulation in MATLAB using the flat spiral spring presented in sub-section 5.4 indicates that the displacement increases with time, which is as expected and reaches a peak value of 5.7 m when the spring energy is exhausted, and the bot stops. The velocity characteristics simulation of the spring given in subsection 5.4 shows that the peak velocity of 1.5 m/s is attained by the turtle bot in 1 second and the velocity is reduced to zero at the 7th second. The TBR used in this research work is based on a validated model using the Euler-Lagrange method. For no load and 10 kg load conditions shown in Fig. 4, the bot could travel an average distance of 4.4 m, whereas for a 20 kg load, the bot could travel only up to 3.8 m. For a 30 kg load, the bot could travel a distance of 3.2 m only, on average. Under various load conditions shown in Fig. 5, the velocity curve exhibits a linearity portion up to 1.2 s for 10 kg and 20 kg loads, whereas the linearity portion extends up to 1.9 s for a 30 kg load. For a 10 kg load, the velocity peaks at 1.7 m/s and for a 20 kg load, it peaks at 1.3 m/s, whereas for a 30 kg load, it is reduced to 1.1 m/s. The roll angle calculated in subsection 5.2 is less than 3.83 degrees, which is well below the recommended roll angle limit, which verifies the stability of the proposed system in case of collision. For a maximum of 3 rotations of the handle by human action, the average force required is 16.06 N as shown in Table 2, which is approximately 33 % of the force that can be exerted by a human hand.

There are some limitations to the proposed flat spiral spring based energy harvesting and utilization method when used in kids' rides compared to that of electrical energy based kids' rides. In the spring based ones, there is no control in terms of the direction and speed of the rides. In addition, these rides cannot last long compared to that of electrical rides, which can be driven for a longer time depending on the availability of electric power. With the current design of the flat spiral spring, the rides can last only for a few seconds. As part of future work, we shall focus on a design mechanism that can increase the energy storage capacity in flat spiral springs so that the rides can be driven for a longer time. In addition, a control mechanism in terms of a steering wheel can be added to the rides so that direction control is available for kids.

7. Conclusions

1. Modeling, analysis and fabrication of TBR, which takes input energy by winding the flat spiral spring, stores in the spring and drives the system are successfully completed. The amount of force a person has to exert in order to wind the spring to the maximum count is also calculated. The average force required to wind the spring is 16.06 N, which is approximately 33 % of the force that can be exerted by a human hand.

2. The impact of the collision between two kid's rides is modeled and analyzed to be safe for kids to drive. The stability of the proposed system in case of collision is verified by calculating the roll angle, which is less than 3.83 degrees, which is well below the recommended roll angle limit in case of collision.

3. An optimum width of 30 mm and a thickness of 1.4 mm for the flat spiral spring are found to help in ease of manufacturability, ease of rotation by human and compactness.

4. The spring specifications are validated using simulations and real-time testing with TBR. The simulation results for distance traveled and velocity of the TBR match with that of the real-time results thereby validating the proposed spring based generation of mechanical energy, which can drive the ride instead of electricity, which is clean and doesn't generate greenhouse gasses.

Conflict of interest

The authors declare that they have no conflict of interest in relation to this research, whether financial, personal, authorship or otherwise, that could affect the research and its results presented in this paper.

Financing

The study was performed without financial support.

Data availability

Data will be made available on reasonable request.

Acknowledgments

The authors thank the Humanitarian Labs and the Department of Electronics and Communication of Amrita Vishwa Vidyapeetham, Amritapuri, Kollam for providing all the necessary lab facilities, and a highly encouraging work environment, which were key factors towards completion of this research project.

References

1. Indian Amusement Park Industry. Insight Alpha. Available at: https://insightalpha.com/news_details.php?cid=81&sid=11&nid=402
2. Wang, J. C., Wang, Y.-C., Ko, L., Wang, J. H. (2017). Greenhouse gas emissions of amusement parks in Taiwan. Renewable and Sustainable Energy Reviews, 74, 581–589. doi: https://doi.org/10.1016/j.rser.2017.02.070
3. Fan, F. R., Tang, W., Wang, Z. L. (2016). Flexible Nanogenerators for Energy Harvesting and Self-Powered Electronics. Advanced Materials, 28 (22), 4283–4305. doi: https://doi.org/10.1002/adma.201504299
4. Guo, L., Lu, Q. (2017). Potentials of piezoelectric and thermoelectric technologies for harvesting energy from pavements. Renewable and Sustainable Energy Reviews, 72, 761–773. doi: https://doi.org/10.1016/j.rser.2017.01.090
5. Donelan, J. M., Li, Q., Naing, V., Hoffer, J. A., Weber, D. J., Kuo, A. D. (2008). Biomechanical Energy Harvesting: Generating Electricity During Walking with Minimal User Effort. Science, 319 (5864), 807–810. doi: https://doi.org/10.1126/science.1149860
6. Abdelkareem, M. A. A., Xu, L., Ali, M. K. A., Elagouz, A., Mi, J., Guo, S. et al. (2018). Vibration energy harvesting in automotive suspension system: A detailed review. Applied Energy, 229, 672–699. doi: https://doi.org/10.1016/j.apenergy.2018.08.030
7. Guo, H., He, X., Zhong, J., Zhong, Q., Leng, Q., Hu, C. et al. (2014). A nanogenerator for harvesting airflow energy and light energy. J. Mater. Chem. A, 2 (7), 2079–2087. doi: https://doi.org/10.1039/c3ta14421f
8. Jiang, T., Zhang, L. M., Chen, X., Han, C. B., Tang, W., Zhang, C. et al. (2015). Structural Optimization of Triboelectric Nanogenerator for Harvesting Water Wave Energy. ACS Nano, 9 (12), 12562–12572. doi: https://doi.org/10.1021/acsnano.5b06372
9. de Araujo, M. V. V., Nicoletti, R. (2015). Electromagnetic harvester for lateral vibration in rotating machines. Mechanical Systems and Signal Processing, 52-53, 685–699. doi: https://doi.org/10.1016/j.ymssp.2014.07.025
10. Ting, C.-C., Tsai, D.-Y., Hsiao, C.-C. (2012). Developing a mechanical roadway system for waste energy capture of vehicles and electric generation. Applied Energy, 92, 1–8. doi: https://doi.org/10.1016/j.apenergy.2011.10.006
11. Trinh, V. L., Chung, C. K. (2018). Harvesting mechanical energy, storage, and lighting using a novel PDMS based triboelectric generator with inclined wall arrays and micro-topping structure. Applied Energy, 213, 353–365. doi: https://doi.org/10.1016/j.apenergy.2018.01.039
12. Li, X., Chen, C., Li, Q., Xu, L., Liang, C., Ngo, K. et al. (2020). A compact mechanical power take-off for wave energy converters: Design, analysis, and test verification. Applied Energy, 278, 115459. doi: https://doi.org/10.1016/j.apenergy.2020.115459
13. Halim, M. A., Rantz, R., Zhang, Q., Gu, L., Yang, K., Roundy, S. (2018). An electromagnetic rotational energy harvester using sprung eccentric rotor, driven by pseudo-walking motion. Applied Energy, 217, 66–74. doi: https://doi.org/10.1016/j.apenergy.2018.02.093
14. Xue, T., Yeo, H. G., Trolier-McKinstry, S., Roundy, S. (2018). Wearable inertial energy harvester with sputtered bimorph lead zirconate titanate (PZT) thin-film beams. Smart Materials and Structures, 27 (8), 085026. doi: https://doi.org/10.1088/1361-665x/aad037
15. von Buren, T., Mitcheson, P. D., Green, T. C., Yeatman, E. M., Holmes, A. S., Troster, G. (2006). Optimization of inertial micropower Generators for human walking motion. IEEE Sensors Journal, 6 (1), 28–38. doi: https://doi.org/10.1109/jsen.2005.853595

16. Mi, J., Li, Q., Liu, M., Li, X., Zuo, L. (2020). Design, modelling, and testing of a vibration energy harvester using a novel half-wave mechanical rectification. Applied Energy, 279, 115726. doi: https://doi.org/10.1016/j.apenergy.2020.115726
17. Wu, F., Li, C., Yin, Y., Cao, R., Li, H., Zhang, X. et al. (2018). A Flexible, Lightweight, and Wearable Triboelectric Nanogenerator for Energy Harvesting and Self-Powered Sensing. Advanced Materials Technologies, 4 (1), 1800216. doi: https://doi.org/10.1002/admt.201800216
18. Cao, S., Li, J. (2017). A survey on ambient energy sources and harvesting methods for structural health monitoring applications. Advances in Mechanical Engineering, 9 (4), 168781401769621. doi: https://doi.org/10.1177/1687814017696210
19. Megalingam, R. K., Nair, L. M., Viswanath, M., Sugathan, S. (2012). Pedalite: Lighting up Lives in Un-electrified Villages. 2012 IEEE Global Humanitarian Technology Conference. doi: https://doi.org/10.1109/ghtc.2012.61
20. Megalingam, R. K., Gedela, V. V. (2017). Solar powered automated water pumping system for eco-friendly irrigation. 2017 International Conference on Inventive Computing and Informatics (ICICI). doi: https://doi.org/10.1109/icici.2017.8365208
21. Prabhu, R. S., Vasudev, O. P. N., Nandu, V., Lokesh, K. J., Anudev, J. (2018). Design and Implementation of A Power Conversion System On A Bicycle With Utilisation By Sensors. 2018 2nd International Conference on I-SMAC (IoT in Social, Mobile, Analytics and Cloud) (I-SMAC)I-SMAC (IoT in Social, Mobile, Analytics and Cloud) (I-SMAC). doi: https://doi.org/10.1109/i-smac.2018.8653679
22. Bhargavi, P., Likhtih, S., Mohanty, A., Mahalakshmi, R. (2021). Design and Power Flow Control in TCSC Compensated SCIG based Wind Energy Conversion Systems. 2021 5th International Conference on Electronics, Communication and Aerospace Technology (ICECA). doi: https://doi.org/10.1109/iceca52323.2021.9675974
23. Zou, H.-X., Zhao, L.-C., Gao, Q.-H., Zuo, L., Liu, F.-R., Tan, T. et al. (2019). Mechanical modulations for enhancing energy harvesting: Principles, methods and applications. Applied Energy, 255, 113871. doi: https://doi.org/10.1016/j.apenergy.2019.113871
24. Evans, V. (2020). Newton's Laws, G-forces and the impact on the brain. Australasian Journal of Neuroscience, 30 (1), 24–29. doi: https://doi.org/10.21307/ajon-2020-003
25. Chen, J.-S., Chen, I.-S. (2015). Deformation and vibration of a spiral spring. International Journal of Solids and Structures, 64-65, 166–175. doi: https://doi.org/10.1016/j.ijsolstr.2015.03.022